IMAV2017-9
https://www.imavs.org/pdf/imav.2017.9

Application of Lattice Boltzmann Method to some challenges related to Micro Air Vehicles

Nicolas Gourdain*, Thierry Jardin, Ronan Serre, Sébastien Prothin and Jean-Marc Moschetta
ISAE-Supaero, 10 av. Edouard Belin, Federal University of Toulouse, France

1 Introduction

Numerical simulation, supported by High Performance Computing (HPC) and experimental validation, led to major breakthroughs in our knowledge of complex physical phenomena and our capability to design innovative technologies. To go beyond the current state of the art, there is still a need to improve our aptitude to deal with complex flow physics, including aerodynamics, aero-acoustics or fluid/structure interactions. Such capabilities are mandatory to address ambitious targets, such as Earth exploration but also the investigations beyond the limit of our planet. Together with the advent of micro-technologies, Micro Air Vehicles (MAVs) recently appeared as a relevant solution for missions of observation and surveillance. MAVs with enhanced endurance and ability to operate in constrained environments would considerably decrease surveillance costs while preserving operators safety in many civilian and military applications. They can also be used in environment where the presence of Humans is not yet possible. However, because of their small dimensions and the intrinsically low Reynolds numbers at which they operate, as well as the difficulty to optimize aerodynamic performance for both forward and hovering flight, current MAVs exhibit relatively low endurance (typically between 15 to 25 minutes in hover) .

Low Reynolds number flows, typical of MAVs ($Re \approx 10^5$), tend to promote flow separations (that decrease efficiency and lift), which are difficult to predict with classical Computational Fluid Dynamics methods, based on a Reynolds Averaged Navier-Stokes (RANS) approach (where all scales of turbulence are modelled). With the increase in computing power, Large Eddy Simulation (LES) emerges as a promising technique to improve the reliability of flow solver predictions [1]. Several works have already show that LES lead to significant improvements both in the understanding of flow physics and performance predictions of rotors [2]. Usually, LES is based on the resolution of the filtered Navier-Stokes equations. While effective, this method require the use of artificial dissipation which limits its accuracy (e.g. transport of turbulence on a long distance, noise predictions, etc.). Lattice-Boltzman Method is a recent and (more and more) popular alternative to such Navier-Stokes flow solvers [3]. Instead of directly solving the Navier-Stokes equations, this method tackles the Boltzmann equation, a statistical equation for the kinetics of gas molecules. Thus, the primitive variables of the LBM represent the statistical particle probability distribution function, to which the usual macroscopic variables pressure and velocity relate as velocity moments, or observables in the sense of statistical mechanics. The particle distribution is a continuous quantity: in contrary to popular believe, the LBM is a continuum method, and not a discrete particle approach. Indeed, the method offers an Eulerian view of the flow and is mesh-based.

To illustrate the advantages and drawbacks of LBM, two applications have been selected in line with MAVs challenges: a rotor operating in-ground effect and new designs to reduce rotor noise. All the LES-LBM simulations have been performed using the open source library Palabos, mainly developed by the University of Geneva.

2 Application to a rotor in-ground effect

This part of the contribution presents numerical investigations undertaken to analyze the turbulent flow produced in the wake of a MAV rotor interacting with the ground [4]. Two configurations are investigated: a free rotor and a shrouded rotor. The Reynolds number based on the chord and tip speed is $Re_{tip} = 0.86 \times 10^5$, which corresponds to a challenging flow where leading edge separations are commonly observed. The numerical simulations are performed with a Reynolds Averaged Navier-Stokes approach and a Large-Eddy Simulation (by means of a Lattice-Boltzmann Method), combined with an immersed boundary approach. The comparison of numerical data with measurements shows that the mean flow and the turbulent shear stresses are accurately predicted close to the ground and in the rotor wake, Fig. 1. However, some discrepancies remain on the prediction of the rotor torque and thrust, mainly due to the difficulty to reproduce the flow near the rotor walls. An analysis is conducted to identify and understand the different sources of turbulent production. The numerical simulations show also that the presence of a shroud contributes, at a given thrust, to reduce the velocity and the turbulent intensity at the ground.

Shrouded rotors usually generate more thrust than equivalent free rotors at a given rotation speed. Therefore, operating at a given total thrust allows reducing

*Email address: nicolas.gourdain@isae.fr

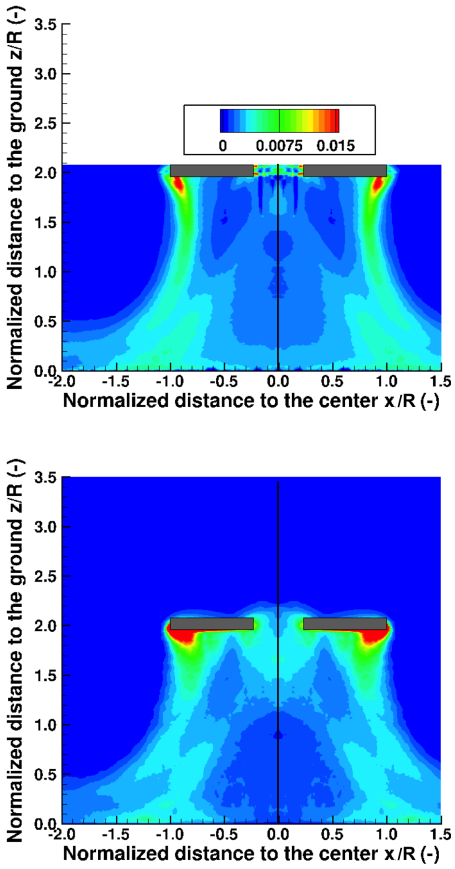

Figure 1: Comparison of the turbulent kinetic energy produced by a MAV rotor in hover, interacting with the ground: (top) measurements and (bottom) LBM prediction.

the part of thrust generated by the rotor itself, hence the rotation speed, thereby reducing the velocity in the rotor wake. In addition, another effect of the shroud is to expand the rotor jet (through a diverging nozzle), which further contributes to decreasing the downward velocity of the rotor wake. All this is conducive to weaker interactions between the rotor and the ground. Ducted and free rotor configurations are compared at a constant rotation rate in Fig. 2. The shroud is responsible for a shift in the location where the rotor wake impacts the ground, that moves from x/R=1.0 (free rotor) to x/R =1.3 (ducted rotor), which corresponds to the effect of the diffuser. No underdeflection is observed at the exit of the diffuser, meaning the boundary layer remains attached despite the adverse pressure gradient. Another effect of the duct is to reduce the thickness of the rotor wake by 20% compared to the free rotor. In the rotor wake ($z/R < 1.5$), the duct reduces the peaks of turbulent kinetic energy (TKE) by 20% and the thickness of the peaks by 50%. The TKE related to the wake mixing in the free rotor case is partially suppressed, which is counterbalanced by a shear layer that develops on the external part of the rotor wake, at the exit of the duct. Close to the ground ($z/R < 0.5$), the turbulent activity remains at the same magnitude order as for the free rotor.

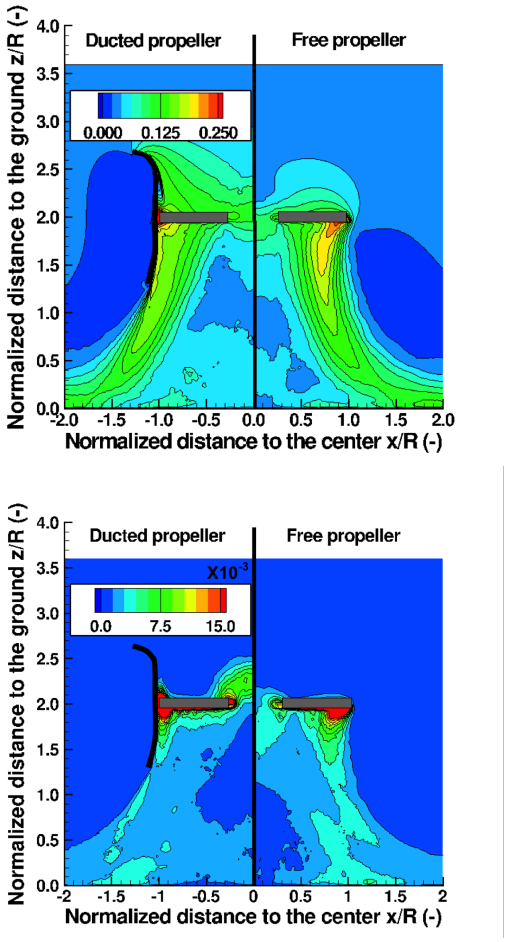

Figure 2: Comparison between a ducted rotor and a free rotor in hover, interacting with the ground: (top) time-averaged velocity flow field and (bottom) time-averaged turbulent kinetic energy flow field.

3 Application to rotor noise

Whether for discretion in military operations or noise pollution in civilian use, noise reduction of MAV is a goal to achieve. Aeroacoustic research has long been focusing on full-scale rotorcrafts. At MAV scales however, the quantification of the numerous sources of noise is not straightforward, as a consequence of the relatively

low Reynolds number that ranges typically from 5,000 to 100,000. Reducing the noise generated aerodynamically in this domain then remains an open topic. This part of the contribution deals with the numerical simulations performed through RANS and LES-LBM to study the flow phenomena that are responsible for the noise generation of a rotor in hover. The initial design is yielded from a low-cost numerical tool developed at ISAE-Supaero based on Blade Element and Momentum Theory (BEMT) for the aerodynamic prediction and formulation of the Ffowcs-Williams and Hawkings (FWH) equation as expressed by [5] coupled with broadband noise models for the acoustic prediction.

Only the global aerodynamic forces are measured with a five components balance. Indeed, the comparison between experimental and numerical predictions is done only for the torque and thrust coefficients, C_Q and C_T, defined as

$$C_T = \frac{T}{\frac{1}{2}\rho(\Omega.R)^2\pi R^2} \; ; \; C_Q = \frac{Q}{\frac{1}{2}\rho(\Omega.R)^2\pi R^3}, \quad (1)$$

with R the radius at the rotor tip. These coefficients are shown in Fig. 3. To check the general shape of the performance curve, another operating point at $\Omega = 314.16 rad.s^{-1}$ (3000 rpm) has been simulated both with URANS and LES-LBM. At 3000 rpm, the accuracy of LES-LBM on thrust is very good (about 1%). Both URANS and BEMT over-predict the thrust coefficient by 15%. When considering the torque coefficient, the order of the methods regarding their accuracy is inverted: LES-LBM, URANS and BEMT over-predicts torque by 50%, 40% and 21%, respectively. At 4950 rpm, similar conclusions can be drawn: the thrust coefficient is under-predicted by 2.5% with LES-LBM, and over-predicted by 14% and 17% by URANS and BEMT, respectively. For the torque, LES-LBM, URANS and BEMT over-predicts it by 29%, 23% and 12%, respectively. It is unclear why three very different numerical methods over-predict the torque (especially the BEMT which neglect 3D effects and predicts fully attached boundary layers). Unfortunately, due to the lack of experimental data, it is not possible at the moment to identify the origin of these discrepancies.

The local thrust coefficient is plotted in Fig. 4 for the three methods. As already shown, BEMT predicts the higher thrust coefficient and LES-LBM the lowest one. From the root to $r/R = 0.4$, the three methods give the same local thrust coefficient. Then, both URANS and LES-LBM predict the same evolution until $r/R = 0.75$ while BEMT already predicts a higher value. All methods show a peak for the thrust coefficient at r/R =0.82 (URANS, LES-LBM) or 0.83 (BEMT). However the values of C_T at the peak are different: C_T=0.19 (LES-LBM), 0.22(URANS) and 0.265 (BEMT). Beyond

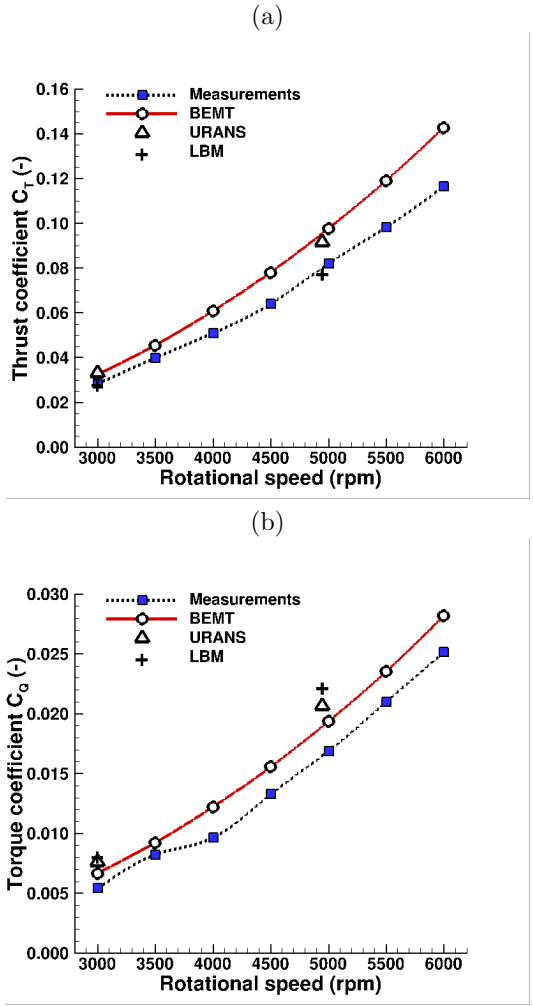

Figure 3: Comparison of global performance: (a) thrust coefficient C_T and (b) torque coefficient C_Q.

$r/R = 0.85$ the value of C_T decreases rapidly. Actually the main conclusion is that the three numerical methods agree reasonably well on a large part of the rotor span, but predict very different behaviour close to the tip.

Three designs are investigated: the reference one, a wavy leading edge design and a design where the blade are shifted along the z-axis. For the three designs, a breakdown of the tip vortex starts close to the trailing edge, due to the recompression. The mixing process between the different vortices produces turbulence that impacts the following blade. A time-averaged flow field, obtained in the reference frame of the rotor, and colored with the normalized fluctuations of pressure $p'/(\frac{1}{2}\rho(\Omega.R)^2)$ is shown in Fig. 5. For the three designs, most of the pressure fluctuations are observed at two locations close to the trailing edge in the vicinity of the

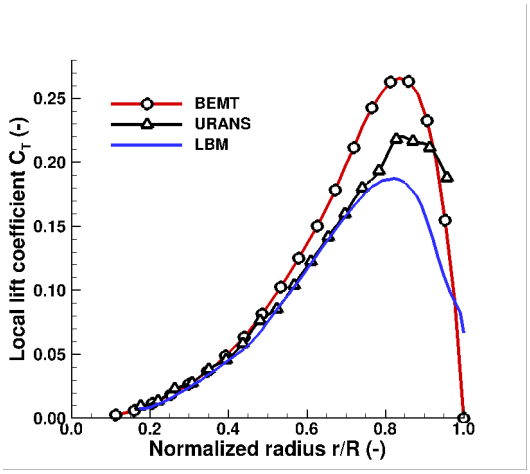

Figure 4: Local thrust coefficient.

rotor tip (tip vortex and suction side separation). The noticeable differences between the three geometries are: 1) for the reference and the wavy leading edge cases, the three blades exhibit the same field of pressure fluctuations, but it is not the case for the shifted blade case (as expected); 2) the source of fluctuations at the rotor tip is reduced with the wavy leading edge; 3) the level of pressure fluctuations in the shifted blade geometry is reduced for two blades (the top-shifted and the middle blade) and is increased for the last one (the bottom-shifted). Compared to the reference geometry, the shifted blade reduces the source at the leading edge but it has a detrimental impact on the trailing edge source.

The global noise of each configuration can be evaluated at a distance of 10 rotor radii, by integrating the pressure signal on all frequencies, which gives a total noise of 1) 64.9dB (reference geometry), 2) 64.1 dB (wavy leading edge) and 3) 68.4 dB (shifted blade).

4 Conclusion

This works shows that LES-LBM has a very good capability to describe the flow around rotors for MAVs applications, both regarding velocity and turbulence. The torque and thrust are also correctly predicted, despite the complexity of the flow (tip vortex, boundary layer separations), with an accuracy close to RANS. Regarding the understanding of flow physics, LES-LBM shows that turbulence is mainly produced by the tip vortex. For a rotor approaching the ground, the slowdown and redirection of the rotor wake is responsible for an intense production of turbulence. Different designs have been investigated to reduce the far-field noise emitted by the rotor. Among the solutions tested, the use of a wavy leading edge is a promising approach to reduce noise. Further investigations should now investigate the poten-

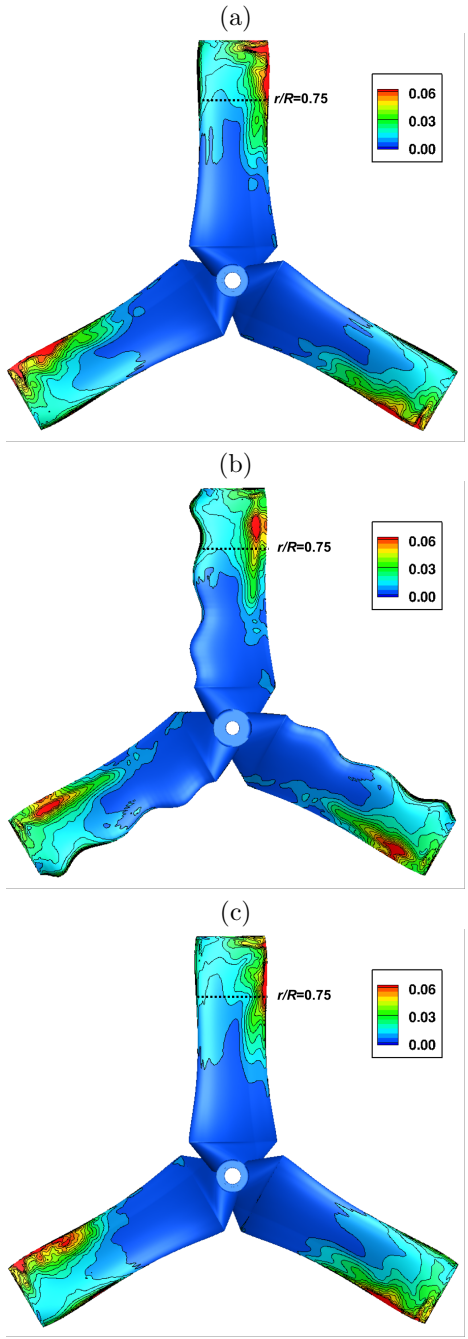

Figure 5: Time-averaged solution on the suction side colored by the normalized pressure fluctations $p'/(\frac{1}{2}\rho(\Omega.R)^2)$: (a) reference geometry, (b) wavy leading edge and (c) shifted blades.

IMAV2017-9
https://www.imavs.org/pdf/imav.2017.9

tial of LES-LBM to describe near wall flows and further experimental campaigns are still mandatory to validate the predictions obtained with the LES-LBM technique.

Acknowledgements

Numerical simulations have been performed thanks to the computing center of the Federal University of Toulouse (CALMIP, project p1425) and resources provided by GENCI. These supports are greatly acknowledged. Special thanks to the technical team of DAEP at ISAE-Supaero for the acquisition of experimental data and to Orestis Malaspinas and Jonas Latt, from the University of Geneva, for their support on Palabos. The authors also thank CERFACS, for providing the software used for post-processing and ONERA for the collaborative work on-going around unmanned aerial vehicles.

References

[1] W. Wu and U. Piomelli. Reynolds-averaged and wall-modelled large-eddy simulations of impinging jets with embedded azimuthal vortices. *European J. of Mechanics – B/Fluids*, 55(2), 2016.

[2] R. Ghias, R. Mittal, H. Dong, and T. Lund. Large-eddy simulation of the tip flow of a rotor in hover. In *34th AIAA Fluid Dynamics Conference and Exhibit*, number paper 2004-2432, 2004.

[3] P. Lallemand and L. S. Luo. Theory of the lattice boltzmann method: dispersion, dissipation, isotropy, galilean invariance, and stability. *Phys. Rev. E*, 61(6), 2000.

[4] N. Gourdain, D. Singh, T. Jardin, and S. Prothin. Lattice boltzmann simulation and analysis of the turbulent wake of a mav hovering near the ground. In *European Rotorcraft Forum*, 2016.

[5] F. Farassat. Theory of noise generation from moving bodies with an application to helicopter rotors. In *NASA Tech. Report*, volume R-451, 1975.